Supporting Information

Electronic structures engineering of single atomic Ru by Ru nanoparticles to enable enhanced activity for alkaline water reduction

*Qi Hu[#], Guomin Li[#], Xiaowan Huang, Ziyu Wang, Hengpan Yang, Qianling Zhang, Jianhong Liu, Chuanxin He**

College of Chemistry and Environmental Engineering, Shenzhen University, Shenzhen, Guangdong, 518060, People's Republic of China.

*To whom correspondence should be addressed. Email: hecx@szu.edu.cn (C. He)

Table S1 Chemical compositions of PC determined by Elemental analysis

Samples	Weight (wt%)			
	C	N	O	H
PC	91.5	1.1	2.8	1.0

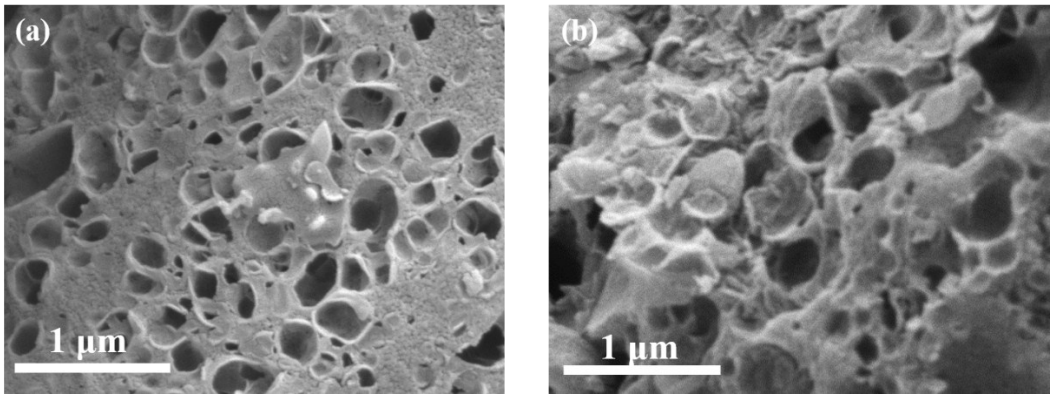

Figure S1 SEM images of the porous N-doped carbon (denoted PC) derived from litchi pericarps.

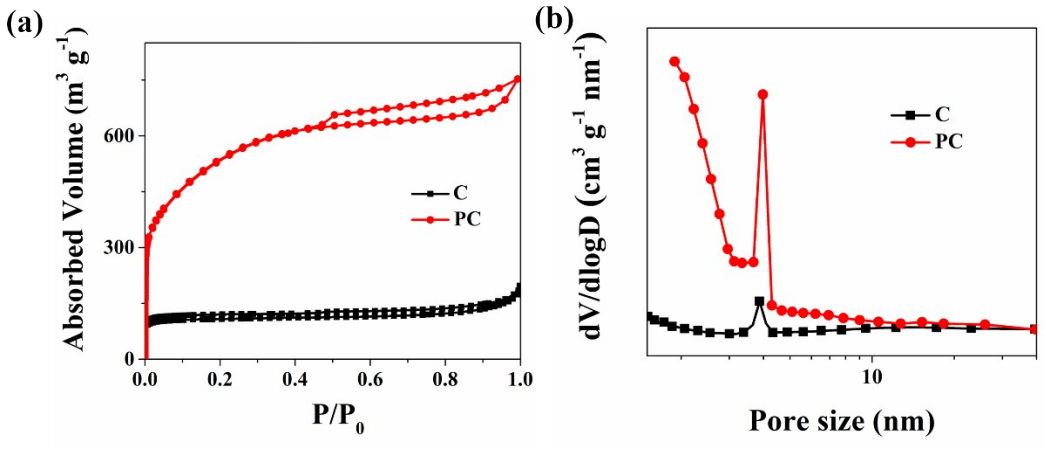

Figure S2 (a) N_2 adsorption-desorption isotherms of C (without hierarchical porous nanostructures) and PC (with hierarchical porous nanostructures), (b) corresponding pore distribution of above two samples based on a method of Barrett-Joyner-Halenda (BJH).

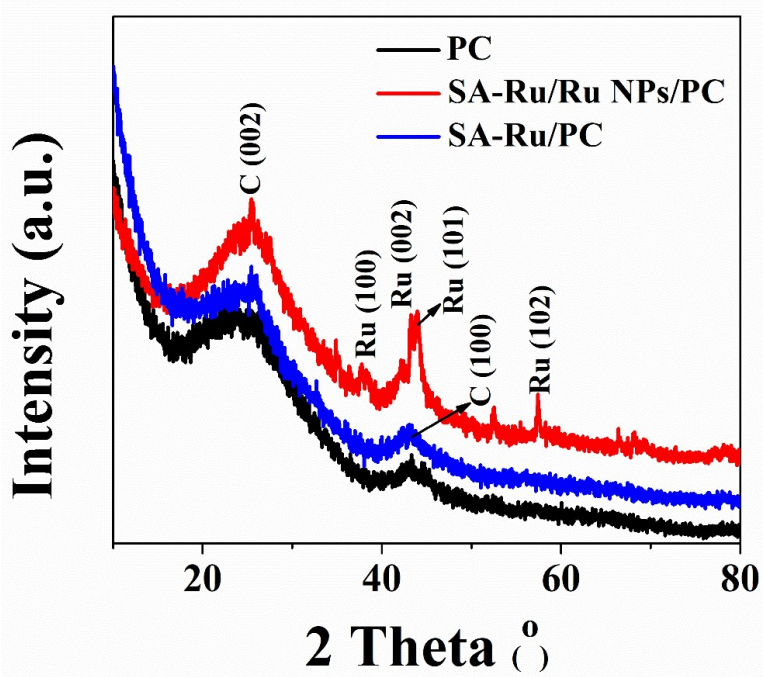

Figure S3 XRD patterns of PC (without SA-Ru or Ru NPs), SA-Ru/Ru NPs/PC (with both SA-Ru and Ru NPs), and SA-Ru/PC (with only SA-Ru).

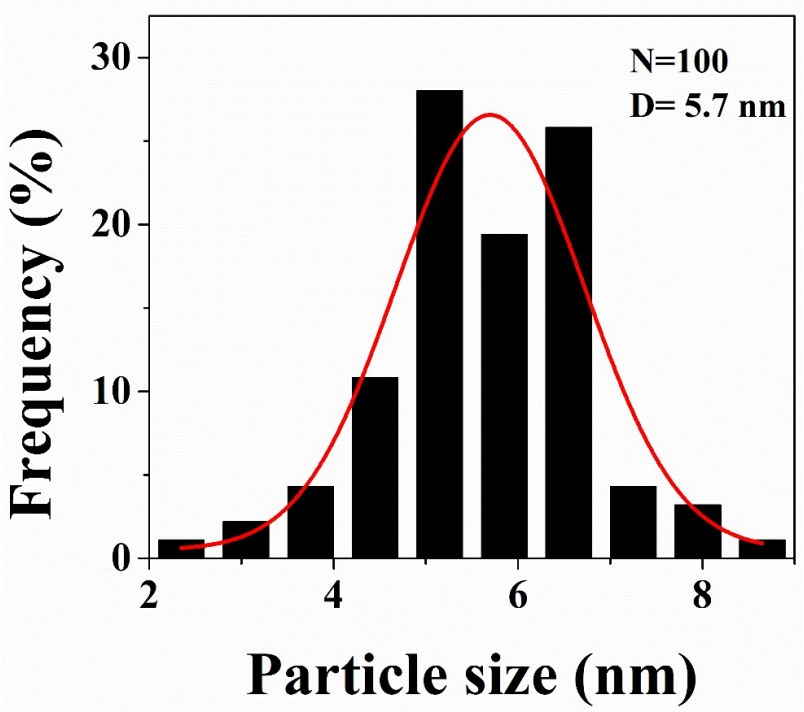

Figure S4 Size distribution of Ru nanoparticles (NPs) on the SA-Ru/Ru NPs/PC.

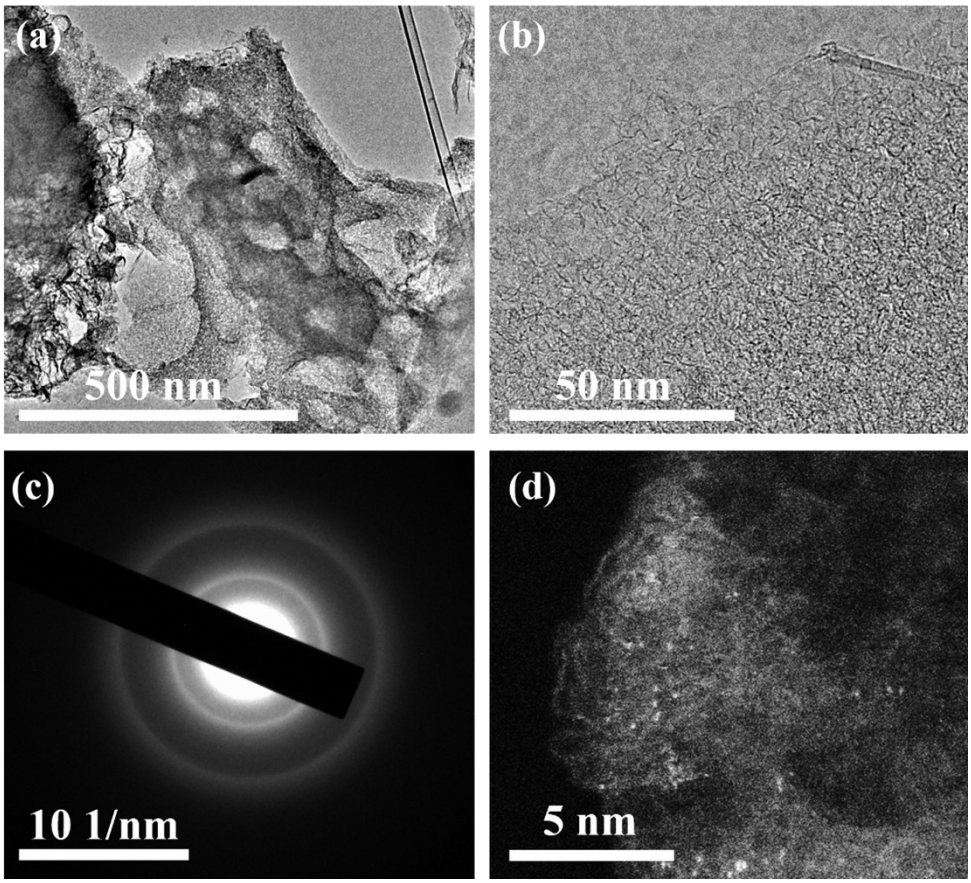

Figure S5 (a, b) TEM image of SA-Ru/PC (without Ru NPs but with SA-Ru), (c) select-area electron diffraction (SAED) images of SA-Ru/PC, (d) STEM-HADDF images of SA-Ru/PC.

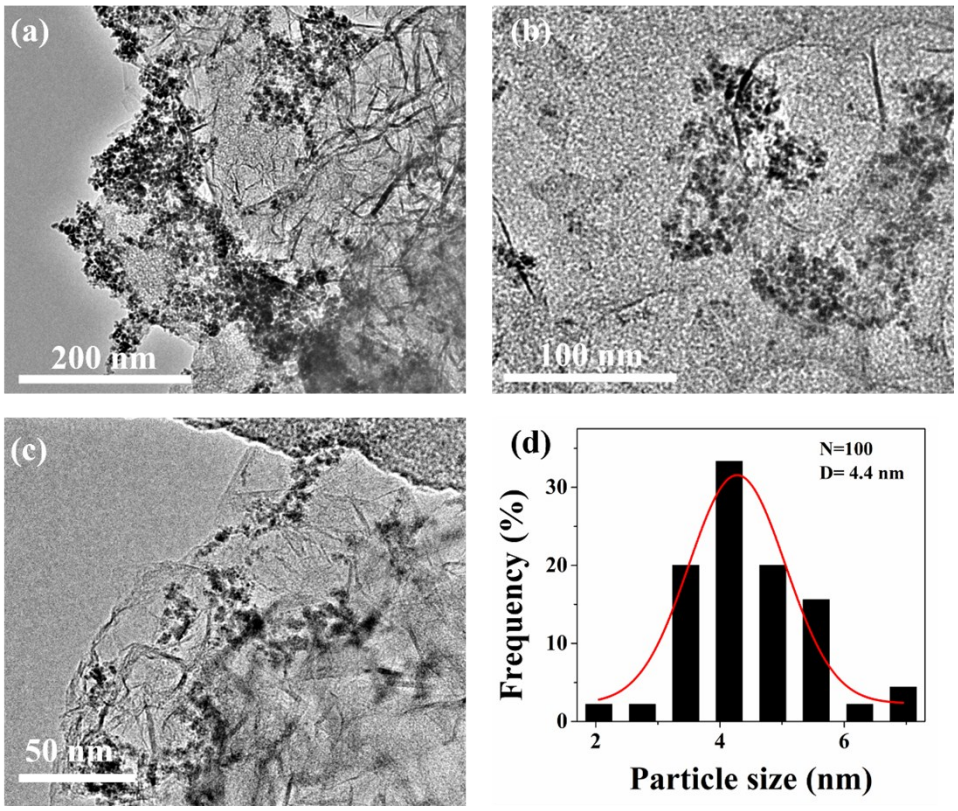

Figure S6 (a, b, c) TEM images of Ru NPs/PC (without SA-Ru but with Ru NPs), (d) size distribution of Ru NPs on the Ru NPs/PC.

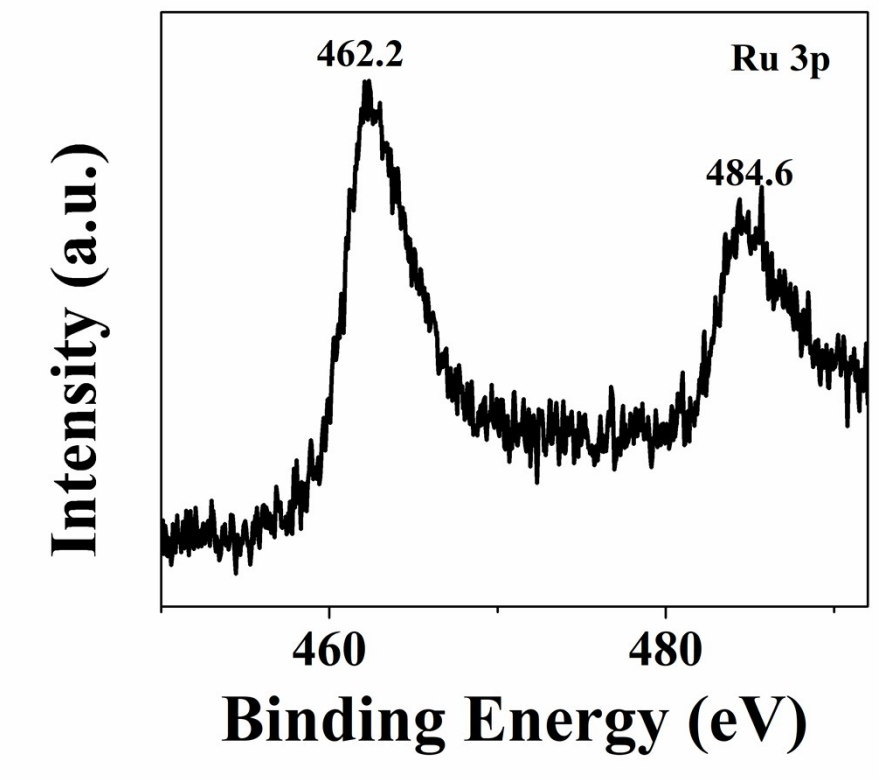

Figure S7 Ru 3p XPS spectra of Ru NPs/PC.

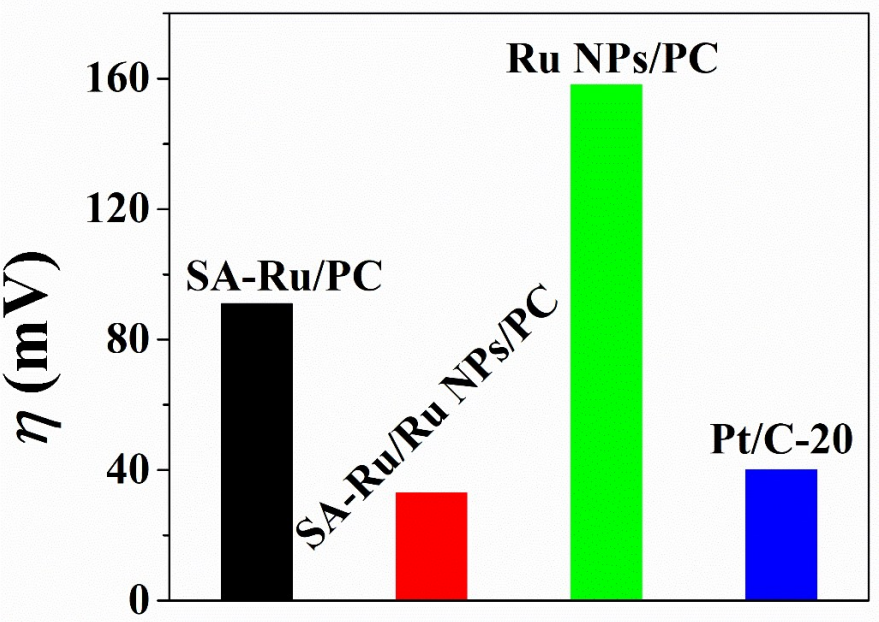

Figure S8 Overpotentials of SA-Ru/PC, SA-Ru/Ru NPs/PC, Ru NPs/PC, and Pt/C-20 at the current density of 10 mA cm^{-2}.

Table S2 Comparison of HER activity with recent reported literatures

Electrocatalysts	Mass loading (mg cm^{-2})	Current density (mA cm^{-2})	Overpotential at certain *j* (mV)	Tafel slope (mV dec^{-1})	Reference
SA-Ru/Ru NPs/PC（2.4 wt%）	0.4 (Ru: 9.6 μg cm^{-2})	10 20 100	33.0 45.0 65.1	31.8	This work
Ru/C_3N_4/C (20 wt%)	0.2 (Ru: 40 μg cm^{-2})	10	79	N/A	1
Ru@C_2N (28.7 wt%)	0.285 (Ru: 82 μg cm^{-2})	10 20	17 35.5	38	2
RuCo@NC	0.275	10 100	28 218	31	3
Ru@NC (2 wt%)	0.3 (Ru: 6 μg cm^{-2})	10 20 100	26 40 98	36	4
Ru-NC-700 nanowires	0.2	10	12	14	5
Porous Ru nanomaterials	0.36 (Ru: 360 μg cm^{-2})	10	83	80	6
RuP_2@NPC	1.0	10	52	69	7
Ni1.5Co1.4P@Ru	0.25	10 50	52 105	50	8

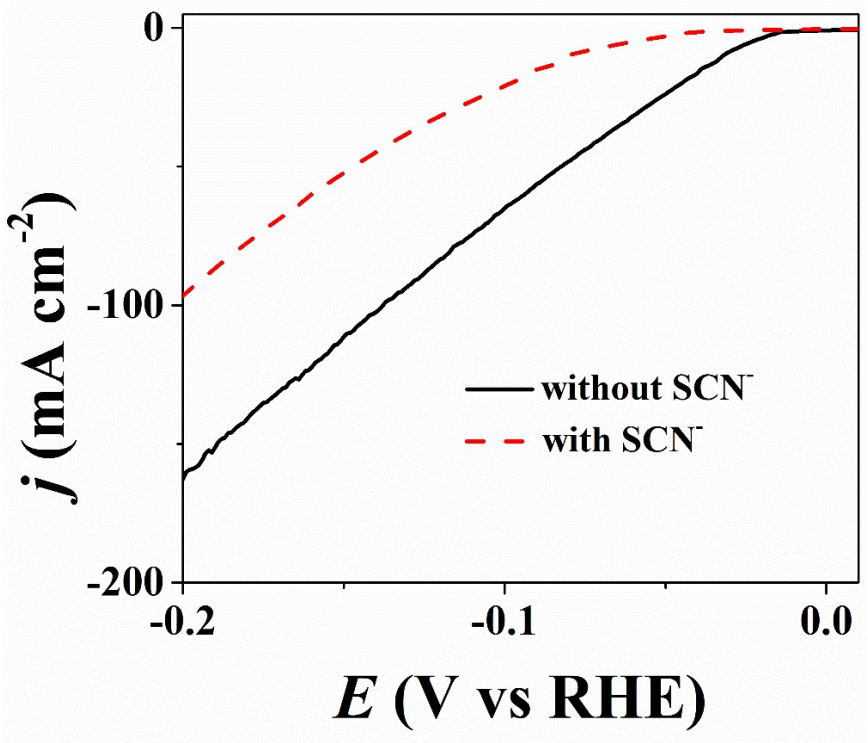

Figure S9 LSV curves of SA-Ru/Ru NPs/PC with and without addition of 10 mM SCN^- to electrolyte

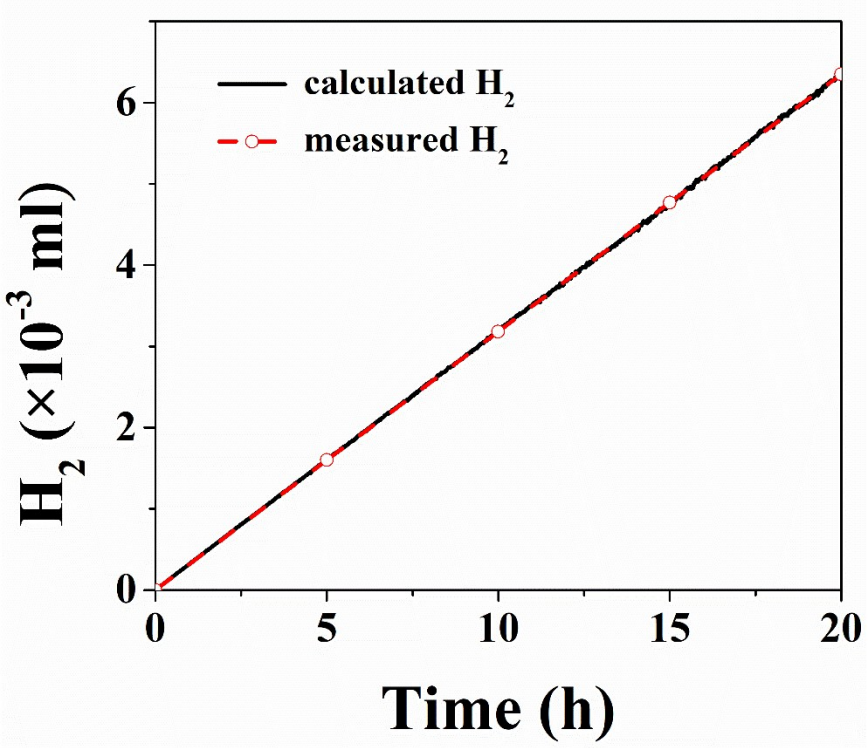

Figure S10 Hydrogen amount theoretically calculated and experimentally measured versus time for SA-Ru/Ru NPs/PC at the potential of -0.07 V vs RHE.

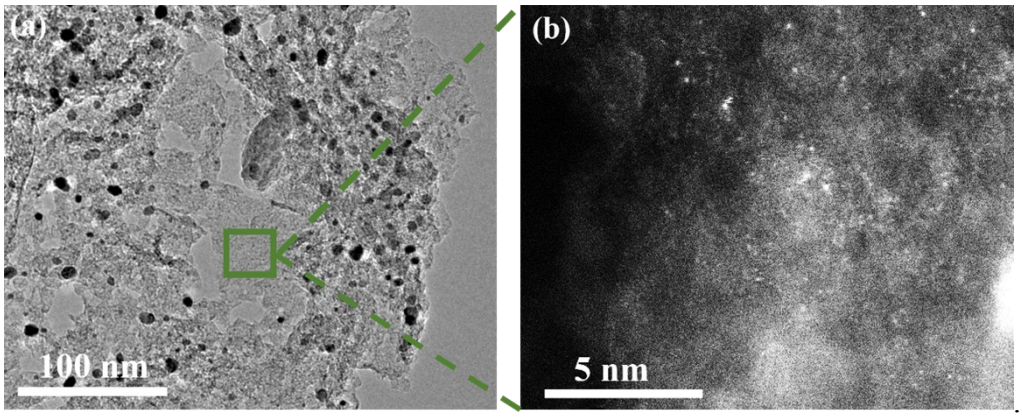

Figure S11 TEM and HADDF-STEM images of SA-Ru/Ru NPs/PC after stability test of 24 h.

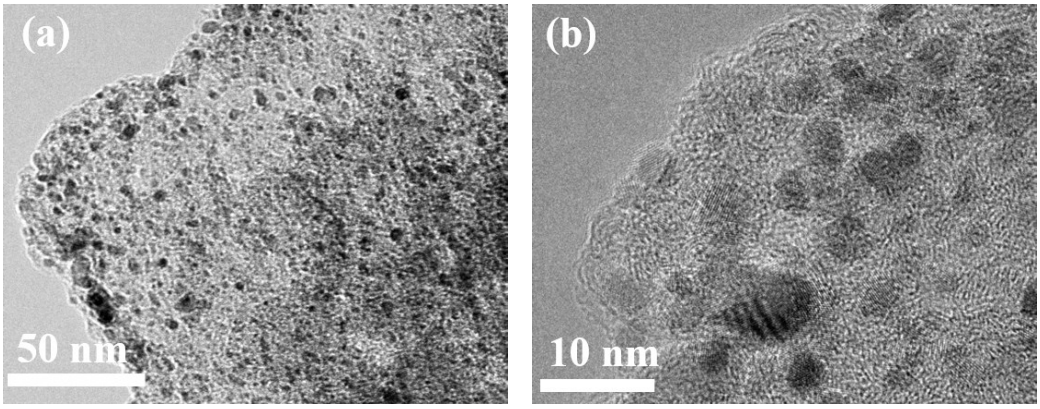

Figure S12 TEM images of SA-Ru/Ru NPs/PC (without hierarchical porous nanostructures).

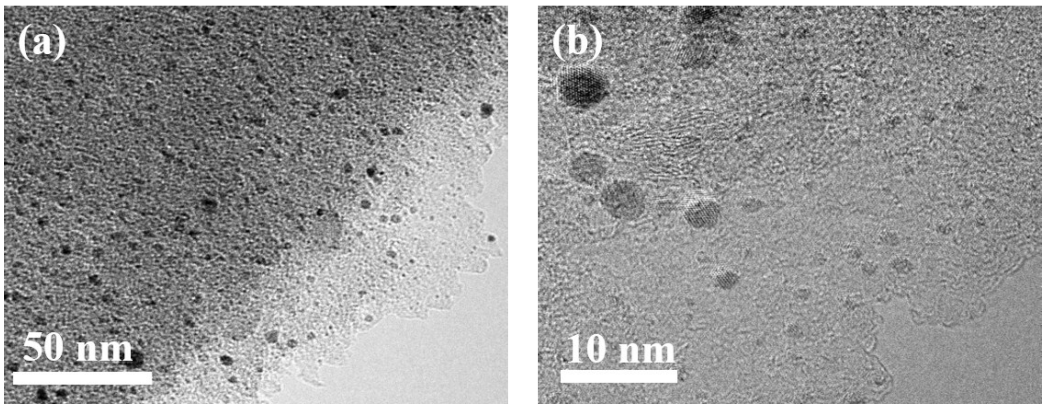

Figure S13 TEM images of Ru/GO (supported on the graphene oxide)

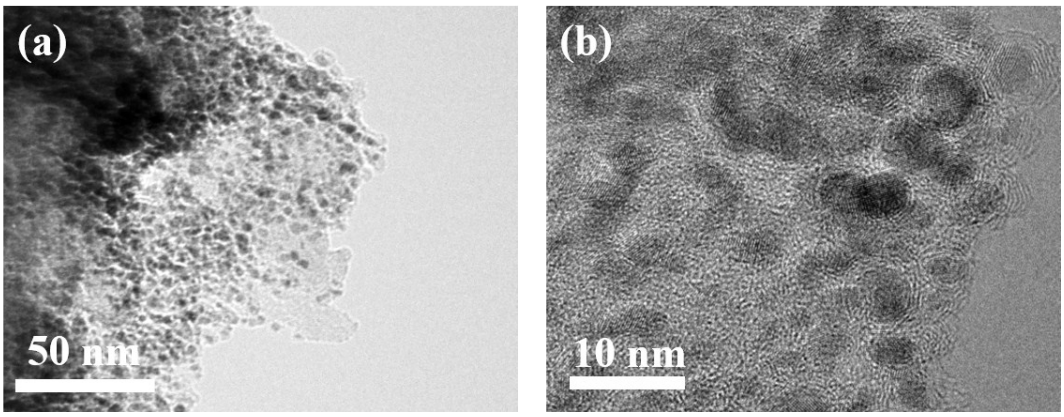

Figure S14 TEM images of Ru/C_3N_4 (supported on the carbon nitride).

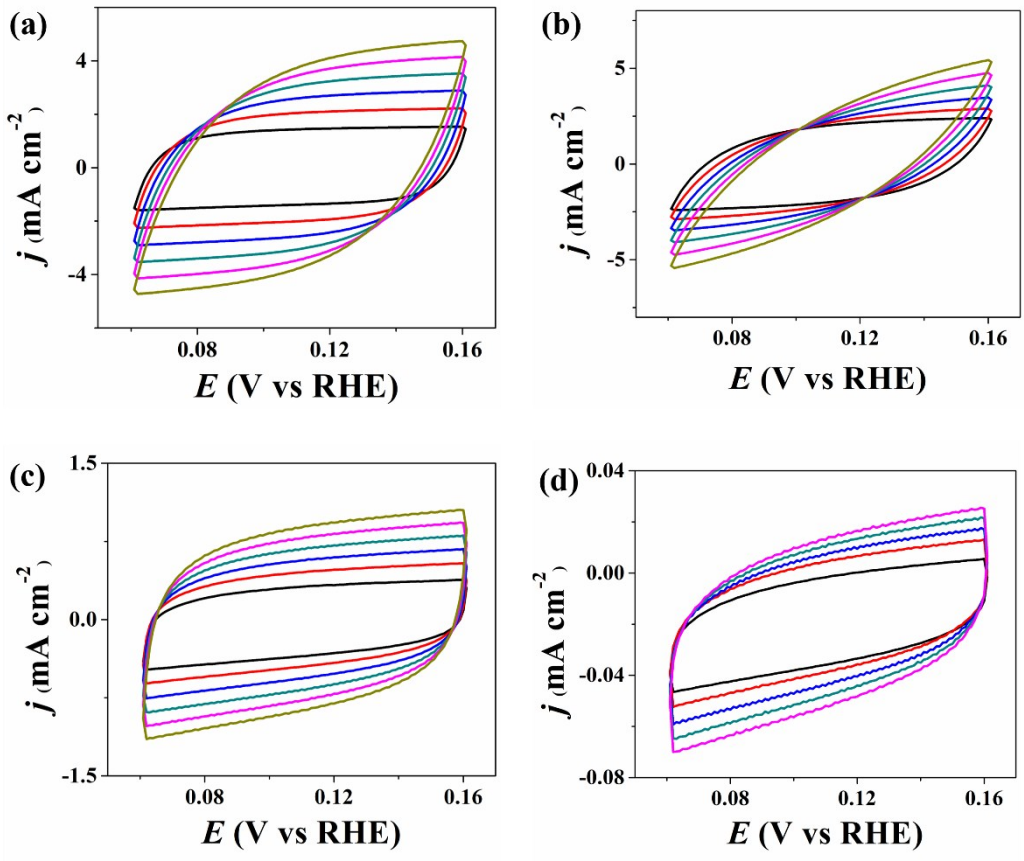

Figure S15 CV curves for (a) SA-Ru/Ru NPs/PC, (b) SA-Ru/Ru NPs/C, (c)Ru/GO, and (d) Ru/C_3N_4 at different rates (i.e. 0.04, 0.06, 0.08, 0.10, 0.12, and 0.14 V/s)

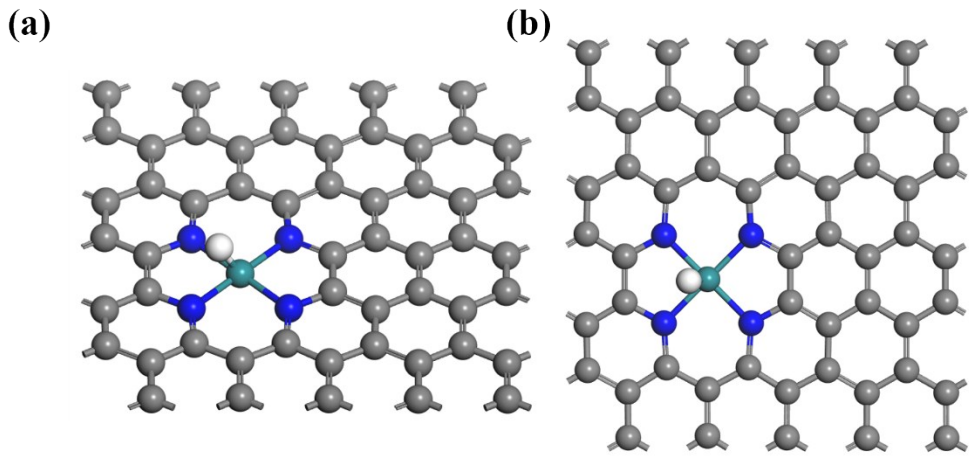

Figure S16 (a) Side and (b) top view of the configuration for H* intermediates absorbed on RuN4. Gray atoms, blue atoms, cyan atoms, and white atoms, represent C, N, Ru, and H elements.

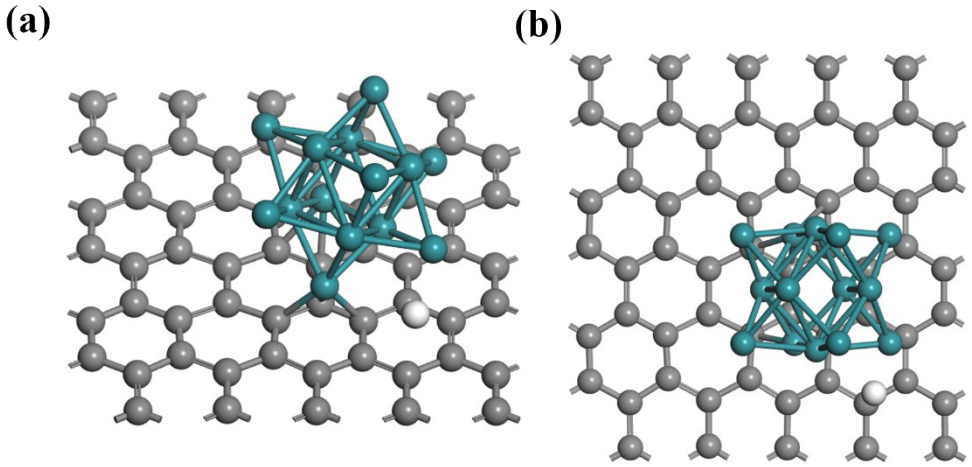

Figure S17 (a) Side and (b) top view of the configuration for H* intermediates absorbed on Ru NPs. Gray atoms, blue atoms, cyan atoms, and white atoms, represent C, N, Ru, and H elements.

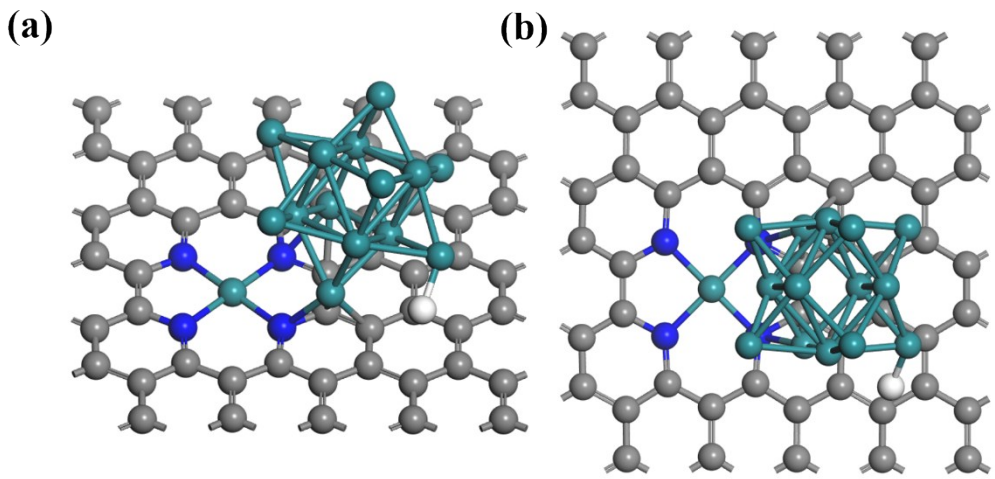

Figure S18 (a) Side and (b) top view of the configuration for H* intermediates absorbed on RuN4/Ru NPs. Gray atoms, blue atoms, cyan atoms, and white atoms, represent C, N, Ru, and H elements.

Reference

1 Zheng, Y., Jiao, Y., Zhu, Y., Li, L. H., Han, Y., Chen, Y., Jaroniec, M., Qiao, S. -Z. High Electrocatalytic Hydrogen Evolution Activity of an Anomalous Ruthenium Catalyst. *J. Am. Chem. Soc.* **2016**, *138*, 16174–16181.

2 Mahmood, J., Li, F., Jung, S. -M., Okyay, M. S., Ahmad, I., Kim, S. -J., Park, N., Jeong, H. Y., Baek, J. -B. An efficient and pH-universal ruthenium-based catalyst for the hydrogen evolution reaction. *Nat. Nanotech.* **2017**, *12*, 441–446.

3 Su, J., Yang, Y., Xia, G., Chen, J., Jiang, P., Chen, Q. Ruthenium-cobalt nanoalloys encapsulated in nitrogen-doped graphene as active electrocatalysts for producing hydrogen in alkaline media. *Nat. Commun.* **2017**, *8*, 14969.

4 Wang, Z. -L., Sun, K., Henzie, J., Hao, X., Li, C., Takei, T., Kang, Y. -M., Yamauchi, Y. Spatially Confined Assembly of Monodisperse Ruthenium Nanoclusters in a Hierarchically Ordered Carbon Electrode for Efficient Hydrogen Evolution. *Angew. Chem. Int. Edit.* **2018**, *57*, 5848–5852.

5 Lu, B., Guo, L., Wu, F., Peng, Y., Lu, J. E., Smart, T. J. Wang, N., Finfrock, Y. Z., Morris, D., Zhang, P., Li, N., Gao, P., Ping, Y., Chen, S. Ruthenium atomically dispersed in carbon outperforms platinum toward hydrogen evolution in alkaline media. *Nat. Commun.* **2019**, *10*, 631.

6 Drouet, S., Creus, J., Amiens, C., García-Antón, J., Sala, X., Philippot, K. A porous Ru nanomaterial as an efficient electrocatalyst for the hydrogen evolution reaction under acidic and neutral conditions. *Chem. Commun.* **2017**, *53*, 11713–11716.

7 Pu, Z., Amiinu, I. S., Kou, Z., Li, W., Mu, S. RuP_2-Based Catalysts with Platinum-like Activity and Higher Durability for the Hydrogen Evolution Reaction at All pH Values. *Angew. Chem. Int. Edit.* 2017, **129**, 11717–11722.

8 Liu, S., Liu, Q., Lv, Y., Chen, B., Zhou, Q., Wang, L., Zheng, Q., Che, C., Chen, C. Ru decorated with NiCoP: an efficient and durable hydrogen evolution reaction electrocatalyst in both acidic and alkaline conditions. *Chem. Commun.* 2017, **53**, 13153–13156.